The Average T–S Relation of a Stochastically Forced Box Model

H. M. STOMMEL

Woods Hole Oceanographic Institution, Woods Hole, Massachusetts

W. R. YOUNG

Scripps Institution of Oceanography, La Jolla, California

18 November 1991 and 5 March 1992

The large-scale T–S relation in the oceanic mixed layer has a density ratio that, in the mean, is close to 2. There are large fluctuations around this average, perhaps due to stochastic forcing such as rainstorms. In this note we study a two-box model of the T–S relation in which the mass exchange between the boxes is a function of the density difference, and the effect of rainstorms is modeled as random precipitation and evaporation. If the random forcing has a decorrelation time much less than the deterministic evolution, then a Fokker–Planck equation can be used to describe the evolution of an ensemble of box models. We find the equilibrium solution of the Fokker–Planck equation and then use it to compute the average density ratio of the ensemble. This average is close to 2, provided that the random fluctuations are large and that the mass exchange is proportional to the absolute value of the density difference between the two boxes. (Other models of the mass exchange lead to different average density ratios.) The effect of forcing with a nonzero time average (e.g., large-scale persistent gradients in precipitation) is assessed, and we conclude that provided the stochastic component of the forcing is sufficiently large, the average density ratio remains near 2.

The vision of the mixed-layer T–S relation, which emerges from this very idealized model, is that enormously variable forcing creates salinity anomalies that are eliminated by some mechanism whose efficacy increases with the density gradient. The combination of large fluctuations and nonlinear mass exchange creates a T–S regulator that holds the average density ratio to values around 2.

1. The box model

The possibility that the observed mean distribution of temperature and salinity in the surface layers of the ocean may be attributed to an interaction between the mean horizontal temperature gradient and the stochastic forcing of random rainfall and evaporation has been raised by Stommel (1992). In this note we explore the process in the simplest of physical systems: two boxes (Fig. 1) connected by orifices at two different levels. The two boxes represent two control volumes at different latitudes in the mixed layer.

Box 1 has temperature fixed at $T_1 = 1$ and box 2 at $T_2 = 0$. The respective salinities are S_1 and S_2 and $y \equiv S_1 - S_2$. We use units so that the density difference between the two boxes is proportional to $(T_1 - T_2) - (S_1 - S_2) = 1 - y$. Conservation of salinity is

$$\dot{S}_1 = \tfrac{1}{2} E(1 - y)(S_2 - S_1) + \tfrac{1}{2} P(t) \quad \text{and}$$

$$\dot{S}_2 = \tfrac{1}{2} E(1 - y)(S_1 - S_2) - \tfrac{1}{2} P(t) \qquad (1.1)$$

where the exchange of mass between the two boxes is modeled by the "exchange function," $E(1 - y)$. A specific model is the form introduced by Stommel (1961)

$$E(1 - y) = |1 - y|. \qquad (1.2)$$

Our principal conclusions do not depend on the detailed structure of the exchange function.

In (1.1) we have included precipitation and evaporation through the forcing function $P(t)$. We denote the long-term mean of this function by μ and write

$$P(t) = \mu + p(t), \qquad (1.3)$$

where the time average of $p(t)$ is zero.

Subtracting the two equations in (1.1) we have a single equation for the salinity difference between the boxes:

$$\dot{y} = -E(1 - y)y + \mu + p(t). \qquad (1.4)$$

Thus, the state of the system is entirely defined by $y(t)$ and the remainder of this note uses (1.4) as the governing equation. Note that the asymmetry between

Corresponding author address: Dr. William Young, Scripps Institution of Oceanography, Mail Code 30, La Jolla, CA 92093.

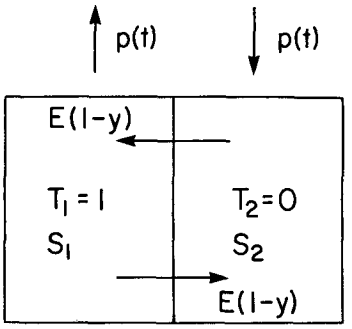

FIG. 1. The two-box model with fixed temperature. The precipitation is $P(t)$ and the salinity difference is $y \equiv S_1 - S_2$. The mass exchange is determined by some function of the density difference $E(1 - y)$.

temperature and salinity in the model is introduced by the assumption that the temperature difference between the two boxes is fixed, while the salinity difference can evolve. In particular, the exchange function E is an even function of the density difference.

If there is no forcing, $\mu = p(t) = 0$, then the system evolves to one of the two steady solutions: $y = 0$ or $y = 1$. If disturbed by a sudden, large positive pulse, say $p(t) = p_0\delta(t - t_0)$, the system jumps to $y = p_0$. There $\dot{y}$ is negative, so y drifts down toward $y = 1$ where it stops. At this point the system is in equilibrium because the density difference is $1 - y = 0$. This is a static state with no mass exchange. But it is a "semistable"[1] equilibrium because even a very small negative jolt moves it to y slightly less than 1, where it again finds $\dot{y} < 0$ and so y drifts away from $y = 1$ toward $y = 0$, where it stops. At this point the system is in equilibrium because there is no salinity difference between the boxes. This equilibrium is linearly stable and has a nonvanishing mass exchange driven by the fixed temperature difference between the boxes.

Note that a large negative pulse drives the system to negative y, where $\dot{y} > 0$, so that the system drifts back to $y = 0$. But in this case there is no semistable equilibrium point to hinder the return to $y = 0$.

If $0 < \mu < \mu_c$ and $p(t) = 0$ then the system has three equilibria: A, B, and C, where A and C are linearly stable and B is linearly unstable. The precise value of μ_c depends on the exchange function $E(1 - y)$. For instance, with the choice in (2), one finds $\mu_c = 1/4$. This is a simplified version of the Stommel (1961) model, which has subsequently been elaborated into climatological models (Bryan 1986; Birchfield 1989; Marotzke 1989). Here we suggest that the Stommel (1961) model can also be used to illustrate the role of lateral thermohaline variations within the mixed layer.

The primary focus of this note is the statistical properties of $y(t)$ when $p(t)$ is a large-amplitude, rapidly changing, stochastic forcing. This drives intermittent reversals of flow between the two boxes and results in sustained and unpredictable time dependence in $y(t)$. We use standard results from statistical physics to obtain the average properties of $y(t)$, but before presenting this theoretical calculation we concretely illustrate the dynamics in (1.4) with a numerical solution.

2. Some numerical examples by time stepping

a. Periodic forcing

Figure 2a shows the results of forcing (1.4) with $\mu = 0$ and

$$p(t) = p_0 \cos(2\pi t). \tag{2.1}$$

The smaller orbit has $p_0 = 2.5$. There is no jump, just a moving phase point, circling the attractor at $y = 0$, but eccentrically with apogee extended toward $y = 1$. This eccentricity is "due to" the other attractor at $y = 1$. In this periodically forced two-box model the analog of the oceanographic "density ratio" ($\alpha\Delta T/\beta\Delta S$ in conventional notation) is $R \equiv 1/\langle y \rangle$ where $\langle y \rangle$ is the average of $y(t)$ over a period. For the small orbit in Fig. 2a $R = 11.7$—a large value. The two larger ovals encircle both attractors. They have p_0 equal to 5 and 10 with $R = 2.4$ and 2.1, respectively. As the amplitude of the forcing increases, $\langle y \rangle$ approaches 1/2, or equivalently R approaches 2. Evidently the attractors at the center of the large-amplitude orbit are so distant that they are seen as a single point at $y = 1/2$.

b. Stochastic forcing

The cloud of points in Fig. 2b corresponds to stochastic forcing of the form $p(t) = 10(\xi - 0.5)$ where ξ is a random number uniformly distributed in the interval $0 < \xi < 1$. ξ is changed at every time step and often it is large enough to alter the sign of the density difference $1 - y$. Once again we find that $R \equiv 1/\langle y \rangle = 2.26$, that is, very close to 2. Thus, it seems not to matter whether the forcing is periodic or stochastic. Provided that the amplitude is large enough the system orbits an "effective attractor" at $y = 1/2$.

3. The Fokker–Planck equation and its equilibrium density

The model in (1.4) is identical to the motion of a particle with no inertia moving in a potential field, $H(y)$, defined by the force law

$$\frac{dH}{dy} = yE(1 - y) - \mu. \tag{3.1}$$

[1] The equilibrium at $y = 1$ is semistable because small positive displacements are exponentially damped, so that y returns to 1, whereas small negative displacements grow exponentially and ultimately take the system to $y = 0$.

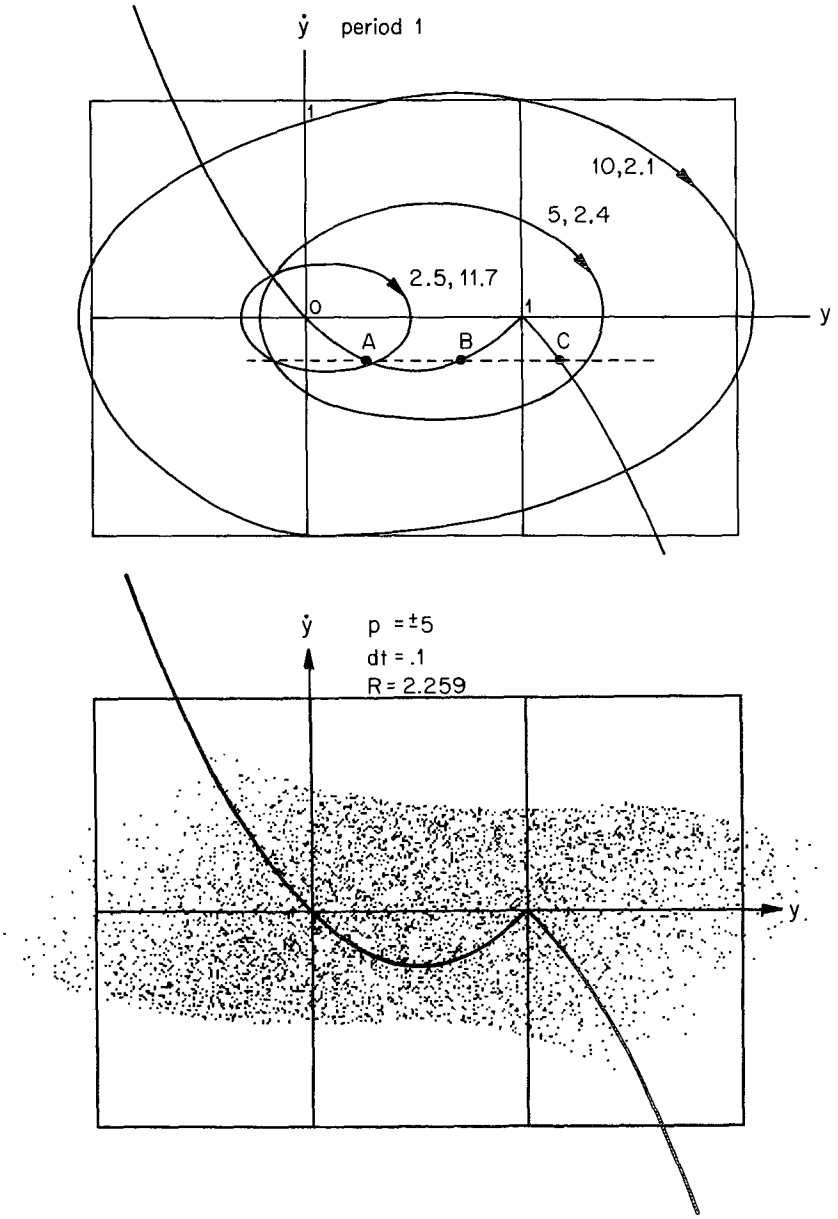

FIG. 2. (a) The $(y, \dot{y})$ plane. The fractured parabola shows that there are two equilibrium states, $y = 0$ and $y = 1$ when $\mu = p(t) = 0$. The state at $y = 0$ is a thermally controlled circulation with no salinity difference. The state at $y = 0$ is a static one with no mass exchange because the density difference vanishes. When $0 < \mu < 1/4$ there are three equilibrium points: A, B, and C, of which B is unstable, the other two corresponding to thermal- and salt-dominated circulations. For $\mu > 1/4$ there is only one equilibrium state—the thermally dominated circulation. Trajectories for periodic $p(t)$ with three sample amplitudes are shown. The labels indicate amplitude and R, respectively. As the amplitude increases the orbit tends to center about $y = 1/2$ so that $R \to 2$. (b) This shows the net result of 1000 random $p(t)$ events [individual points indicate stochastic spread of $(y, \dot{y})$]. The points cluster about $y = 1/2$ leading to $R \approx 2$.

In this analogy $y(t)$ is the position of the particle, $\dot{y}$ is its velocity, $-yE(1 - y) + \mu$ is the deterministic force acting on the particle, and $p(t)$ is the random force due to molecular bombardment. There is no inertia term, such as $m\ddot{y}$, because we suppose that the medium is very resistive (e.g., grains of pollen moving with very small Reynolds number in water). We now introduce the "density of states" $\phi(y, t)$. In an ensemble of re-

alizations of (1), $\phi(y, t)dy$ is the fraction of the ensemble in the interval $(y, y + dy)$. The average of any function of y is

$$\langle f(y, t)\rangle = \int_{-\infty}^{\infty} f(y, t)\phi(y, t)dy. \quad (3.2)$$

If the stochastic forcing has a short decorrelation time (relative to the time scale of the nonstochastic differential equation $\dot{y} = -H_y$), then the evolution of the density function is approximated by the Fokker–Planck equation (e.g., see Wax 1954; Risken 1989; or van Kampen 1984)

$$\phi_t - (H_y\phi)_y = D\phi_{yy}. \quad (3.3)$$

In (3.3) the diffusion coefficient is given in terms of the autocorrelation function of $p(t)$ by Taylor's (1921) formula

$$D = \int_0^{\infty} \langle p(t_0)p(t_0 + t)\rangle dt. \quad (3.4)$$

The critical assumption in approximating the evolution of $\phi(y, t)$ with the Fokker–Planck equation (3.3) is that the correlation function, $\langle p(t_0)p(t_0 + t)\rangle$, decays to zero on a time scale that is much less than that of the deterministic evolution, $\dot{y} = -H_y$.

a. *The equilibrium density*

The equilibrium distribution of y is now found by taking $\phi_t = 0$ and solving the steady-state version of (3.3):

$$\phi_{eq}(y, \alpha, \mu) = \mathcal{N}(\alpha, \mu) \exp(-\alpha H(y, \mu)) \quad (3.5)$$

where $\alpha \equiv 1/D$. The normalization function, $\mathcal{N}(\alpha,\mu)$, is calculated so that

$$1 = \int_{\infty}^{\infty} \phi_{eq}(y, \alpha, \mu)dy. \quad (3.6)$$

The basic idea is that if we start with any initial condition and wait long enough then the ensemble settles into the equilibrium density in (3.5). Note that with the density in (3.5) and the definition in (3.1), the average exchange between the boxes is

$$\langle H_y\rangle = \int_{-\infty}^{\infty} H_y(y)\mathcal{N} \exp(-\alpha H(y))dy = 0. \quad (3.7)$$

Of course this must be true when the system is in equilibrium.

b. *An example*

At this point we adopt the specific model in (1.2) for which

$$H(y, \mu) = \begin{cases} \left(\frac{y^2}{2} - \frac{y^3}{3}\right) - \mu y, & \text{if } y < 1 \\ \left(\frac{1}{3} - \frac{y^2}{2} + \frac{y^3}{3}\right) - \mu y, & \text{if } y > 1. \end{cases} \quad (3.8)$$

Note that $H(1, \mu) = (1/6) - \mu$, that is, both the potential and its derivative are continuous at $y = 1$. In Fig. 3 we plot the potential $H(y, \mu)$ for various values of μ. When $1/4 > \mu > 0$ the potential has a "double well." The two valleys correspond to the stable equilibrium points A and C in Fig. 1, while the peak is the unstable equilibrium point B.

Figure 4 shows the equilibrium density in (3.5) calculated with $H(y, \mu)$ in (3.8) for three values of μ and four of α. When α is small the fluctuations are large and the density function is broad and centered on $\langle y\rangle \approx 1/2$. The structure of the equilibrium density is insensitive to μ. In the complementary limit, when α is small, the fluctuations are weak and the shape of the equilibrium density is sensitive to μ. In particular, when $0 < \mu < 1/4$, the equilibrium density is bimodal.

The averages

$$\langle y^n\rangle = \mathcal{N} \int_{-\infty}^{\infty} y^n \exp(-\alpha H(y))dy \quad (3.9)$$

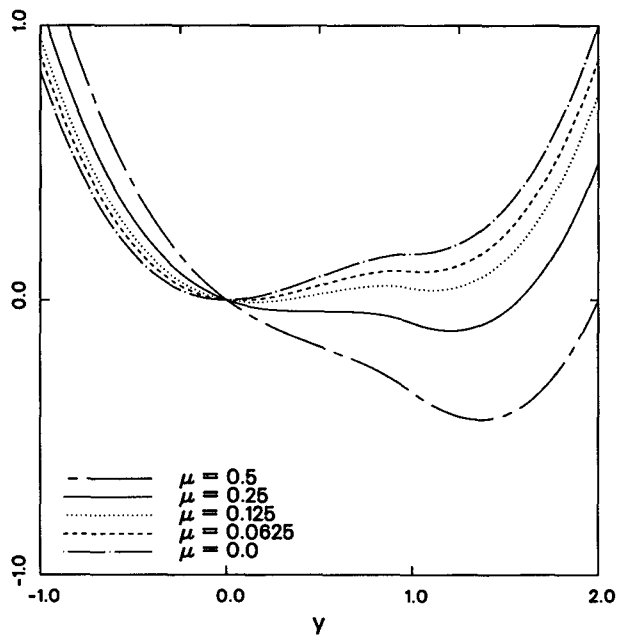

FIG. 3. The potential $H(y, \mu)$ defined in (3.8) for various values of the mean freshwater forcing $\mu = 0$, $1/16$, $1/8$, $1/4$ and $1/2$. When $0 < \mu < 1/4$ the potential has a double well structure because there are two stable equilibrium points.

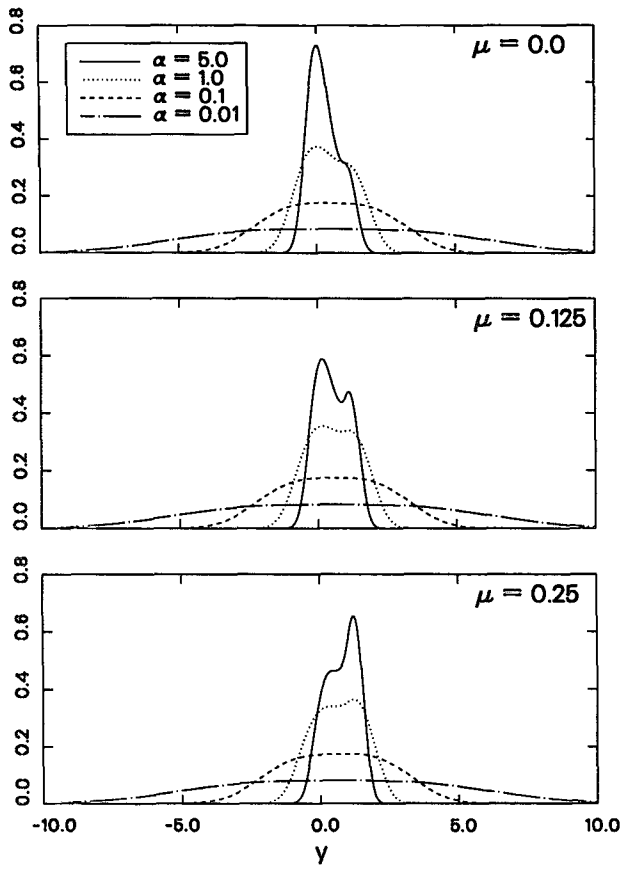

FIG. 4. The normalized equilibrium density, $\phi_{eq}(y, \alpha, \mu)$, computed from (3.5) and (3.8). Each panel shows a different value of μ. Note that when $\alpha \ll 1$ the equilibrium density is insensitive to μ.

can be calculated using numerical quadrature. The results are summarized in Fig. 5 and 6. Figure 5 shows $\langle y \rangle$ as function μ and α. Note that if μ is fixed and $\alpha \to 0$ (i.e., strong fluctuations) then $\langle y \rangle \to 1/2$, so that the density ratio is $R \equiv 1/\langle y \rangle = 2$. Figure 6 shows contours of $\log_{10}\langle y^2 \rangle$ in the μ–α plane. The striking result is that when α becomes small, $\langle y^2 \rangle$ is almost independent of μ.

The assumption $\alpha \ll 1$ (strong fluctuations) can be used to approximate the integrals in (3.9). For simplicity, we also take $\mu = 0$. The results of a tedious calculation are

$$\mathcal{N} \approx \frac{3^{2/3}\alpha^{1/3}}{2\Gamma(1/3)} = 0.388\alpha^{1/3},$$

$$\langle y \rangle \approx \frac{1}{2} - \frac{3^{1/3}\Gamma(2/3)\alpha^{2/3}}{12\Gamma(1/3)} = (1/2) - 0.06075\alpha^{2/3},$$

$$\langle y^2 \rangle \approx \left(\frac{3}{\alpha}\right)^{2/3} \frac{1}{\Gamma(1/3)} = 0.776\alpha^{-2/3}, \quad (3.10)$$

where $\Gamma(z)$ is the gamma function (Abramowitz and Stegun 1972).

The results in (3.10) assume $\alpha \ll 1$ and $\mu = 0$. The complementary limit, $\alpha \gg 1$, is easy because the equilibrium density can be approximated by

$$\phi_{eq} \approx \left(\frac{\alpha}{2\pi}\right)^{1/2} \exp\left[-\frac{\alpha y^2}{2}\right]. \quad (3.11)$$

Thus, in this weak fluctuation limit $\langle y \rangle \approx 0$ and $\langle y^2 \rangle \approx 1/\alpha \ll 1$.

The strong fluctuation case in (3.10) is more relevant to the ocean. In this limit the average density ratio is $R \equiv 1/\langle y \rangle \approx 2$. Note that $\langle y^2 \rangle \sim \alpha^{-2/3} = D^{2/3}$ so that the fluctuations about $\langle y \rangle$ become very large as $D \to \infty$. This is consistent with what is observed in the oceanic mixed layer in the range of latitudes 40° to 55° in both hemispheres of all five major oceanic regions.

We found it interesting to compare the statistics obtained from the equilibrium density in (3.5) with those found from a direct numerical integration. Our numerical scheme is foward Euler:

$$y_{n+1} = y_n - \tau|1 - y_n|y_n + \tau p_n \quad (3.12)$$

where the time step is τ and p_n is a random number uniformly distributed in the interval $-r < p_n < r$. The random number p_n is changed at every time step and so the autocorrelation function is

$$\langle p(t_0)p(t_0 + t)\rangle = \langle p_n^2\rangle\left(1 - \frac{t}{\tau}\right) = \frac{r^2}{3}\left(1 - \frac{t}{\tau}\right). \quad (3.13)$$

Using Taylor's formula for the diffusion coefficient one then has

$$D = \frac{r^2\tau}{6}. \quad (3.14)$$

For accuracy we take a very small value of the time step, say $\tau = 0.01$, and generate a set of y_n from (3.12). By adjusting r, we control the size of the diffusion using (3.14).

Table 1 shows a comparison of this direct simulation with both numerical quadrature of the equilibrium density and the approximations in (3.10). The agreement between the three methods is satisfactory.

c. *Insensitivity to μ when α is small*

One surprising result of these calculations is the weak effect of average forcing ($\mu \neq 0$) when the fluctuations are large. For instance, in Fig. 5b we see that $\langle y \rangle \approx 1/2$, independent of μ, when α is small. The explanation of this insensitivity is the structure $\phi_{eq}(y, \mu, \alpha)$ when α is small. When $0 < \mu < 1/4$ density function in (3.5) has two maxima separated by a minima (see the middle panel in Fig. 4). These three extrema are located

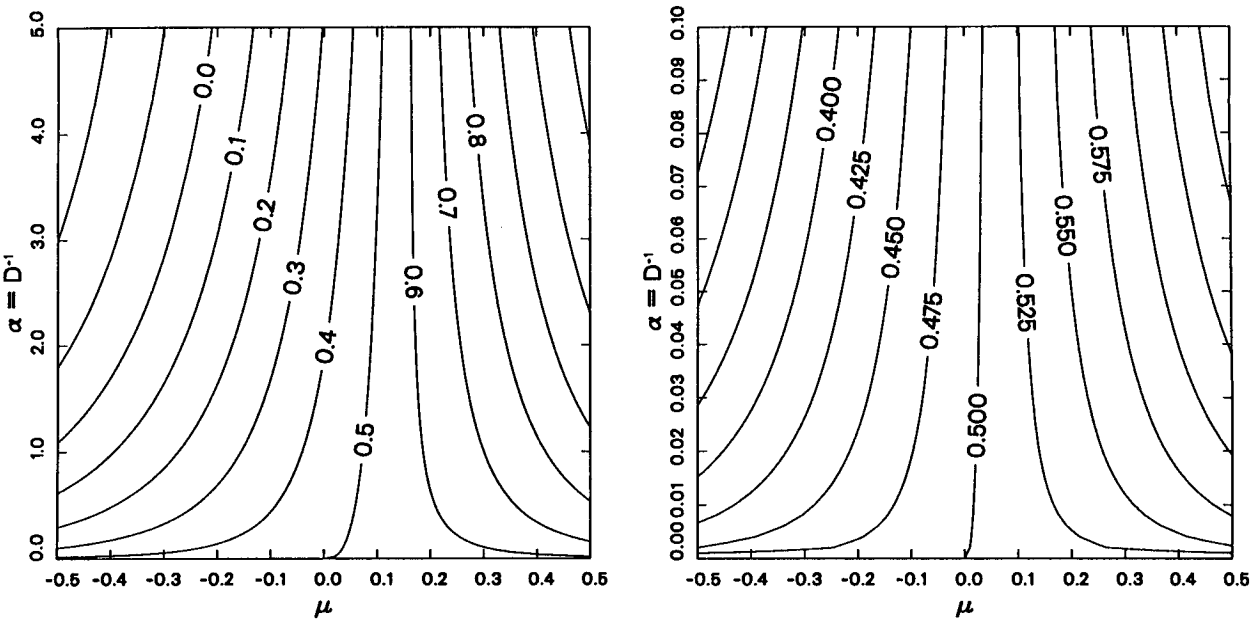

FIG. 5. (a) A contour plot of $\langle y \rangle$ as a function of μ and $\alpha \equiv 1/D$. (b) An expanded view of the region $\alpha \ll 1$. If μ is fixed and $\alpha \to 0$ then $\langle y \rangle \to 1/2$ for all μ.

at the zeros of H_y and correspond to the three equilibrium points A, B, and C in Fig. 2. The unstable point B is the minimum, which falls between the two maxima at A and C. But when $\alpha \ll 1$ the difference in height between these two peaks, and the valley separating them is very small, in fact of order α. Thus, in the limit of large fluctuations the equilibrium density, ϕ_{eq}, has essentially one broad peak, which spans the three points A, B, and C and is centered on $y = 1/2$. This is illustrated in Fig. 4, which contrasts the equilibrium density

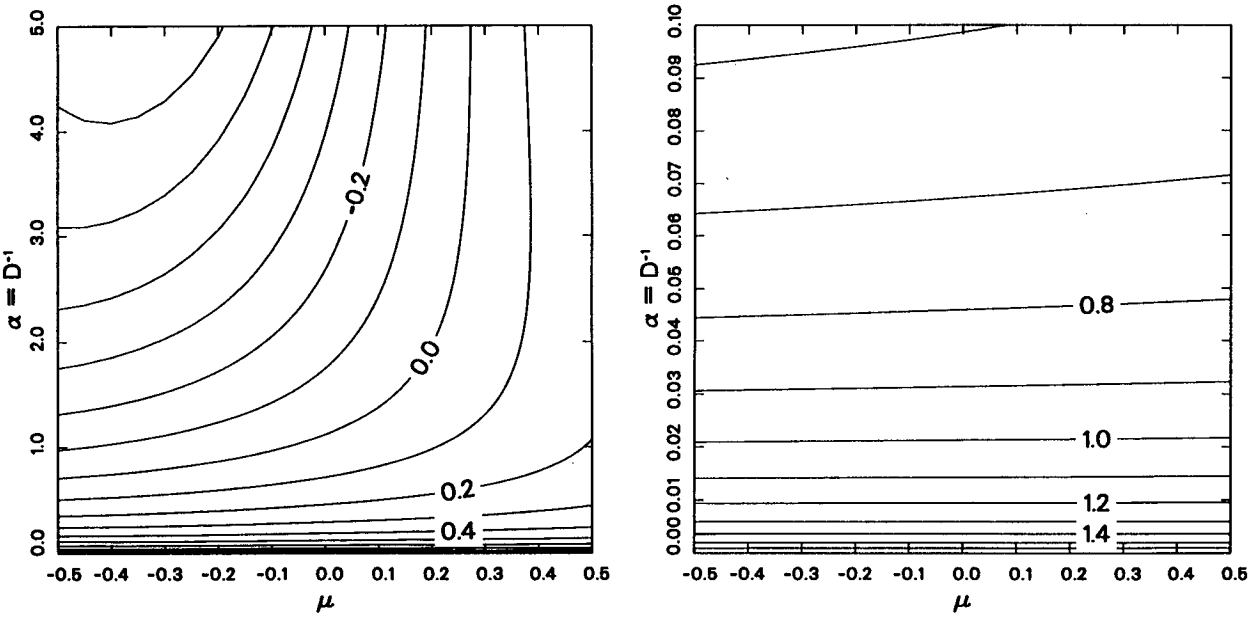

FIG. 6. A contour plot of $\log_{10}\langle y^2 \rangle$ as a function of μ and $\alpha \equiv 1/D$. (b) An expanded view of the region $\alpha \ll 1$ showing that $\langle y^2 \rangle$ is independent of μ as $\alpha \to 0$.

TABLE 1. A comparison of three methods for calculating the statistical properties of the stochastically forced two-box model. In all cases we took $\mu = 0$. Method 1 is direct numerical simulation as described in text. Our time step was $\tau = 0.01$, and we calculated the statistics from a dataset obtained with 10^6 steps. Method 2 is numerical quadrature of the equilibrium density in (3.5) where $H(y)$ is given in (3.8). The averages are calculated using the prescription in (3.9). Method 3 is asymptotic evaluation of the integrals using the assumption that $\alpha \equiv D^{-1} \ll 1$.

Method 1: Direct simulation

r	$D = \tau r^2/6$	$\langle y \rangle$	$\langle y^2 \rangle$
3	0.0150	0.016	0.016
10	0.1667	0.265	0.364
30	1.5000	0.460	1.350
100	16.6667	0.497	5.445

Method 2: Quadrature

D	$\langle y \rangle$	$\langle y^2 \rangle$
0.0150	0.01643	0.01644
0.1667	0.27818	0.37670
1.5000	0.45174	1.32635
16.6667	0.490608	5.41496

Method 3: Asymptotic analysis

D	$\langle y \rangle = 1/2 - 0.06075\alpha^{2/3}$	$\langle y^2 \rangle = 0.776\alpha^{-2/3}$
0.0150	−0.499	0.047
0.1667	0.299	0.235
1.5000	0.453	1.017
16.6667	0.491	5.063

when $\alpha \gg 1$ (two distinct peaks) with the density when $\alpha \ll 1$ (one broad hump).

d. *Estimates of the time required to reach equilibrium*

Using scale analysis, one can estimate the time required to adjust from an arbitrary initial density function [such as $\phi(y, 0) = \delta(y)$] to the equilibrium solution in (3.5). We continue to use the specific form in (3.8) and take $\alpha \ll 1$. The width of the equilibrium density, w, is of order $w \sim \alpha^{-1/3}$ and the time taken to diffuse through this distance is $t_{\text{diff}} \sim w^2/D \sim \alpha^{1/3} \ll 1$. Thus, in the strong fluctuation limit the equilibrium density is rapidly established.

e. *Some comments on different exchange functions*

The results in sections 3b–d were based on the specific exchange function defined in (1.2). With one important exception, our qualitative conclusions are unaltered if we adopt a different model of the exchange function, such as $E(1 - y) = |1 - y|^n$. When the fluctuations are large the average salinity difference, $\langle y \rangle$, is independent of the mean forcing μ. The aforementioned exception is that the value of $\langle y \rangle$ as $D \to \infty$ depends on $E(1 - y)$. For instance with $E(1 - y) = |1 - y|^n$ one finds that $\langle y \rangle \to n/(n + 1)$ as $\alpha \equiv 1/D \to 0$. To explain the observational fact that the observed density ratio $R \equiv 1/\langle y \rangle$ is close to 2, we must take $n = 1$. This coincidence is a very appealing feature of the specific exchange function in (1.2). Justifying this model with a mechanism that is more plausible than the capillary tube analogy of Stommel (1961) is an open question.

f. *The asymmetry of stochastic forcing*

In our computation of D using (3.13) and (3.14) we picked $p(t)$ for simplicity to be statistically symmetrical about $p = 0$. The real nature of $p(t)$ is asymmetrical in the sense that the intervals of rainfall are short and intense, whereas the intervals of evaporation are longer and less intense. The reader will notice, however, that to the order of approximation embodied in the Fokker–Planck equation this asymmetry only modifies the value of D. Once D is known the deductions from the Fokker–Planck equation are independent of asymmetries in $p(t)$.

4. Conclusions

The main result of this study is that the mean difference of salinity between two boxes in a model of density-driven convective circulation tends toward a fixed "critical" value independent of the amplitude and frequency of the stochastic forcing, provided that they are both large enough. If the physics of the convection requires that the amplitude of the circulation be linearly proportional to the density difference, the "critical" value of the mean salinity difference is that required to cancel one-half of the density difference due to the imposed temperature difference. Thus, the average density ratio is 2.

By way of contrast to the aforementioned result for stochastic forcing, if the precipitation and evaporation is changed slowly, so the model moves quasi-statically through a series of equilibria, it is known that there are multiple equilibria. These multiple equilibria exist only if the forcing lies in a certain range [e.g., $0 < \mu < 1/4$ with the exchange function in (1.2)]. At the upper end of this range with multiple states the salinity difference has the same value as the critical value referred to above. Of course the value of the salinity difference in the steady state close to the upper end of the range of multiple states is very sensitive to the amplitude of the forcing, as it is close to the evanescence of the state itself. This is what makes the idea attractive to climatologists seeking sensitivities in their numerical models of the joint ocean–atmosphere system. On the other hand, this sensitivity close to the observed salinity difference suggests that the amplitude of freshwater forcing in a steady model requires a tuning exquisite beyond

our present knowledge of its actual amplitude and geographical distribution.

For those interested in a possible explanation of the observed fact that the observed state of the oceanic mixed layer is close to the critical mean state as defined by the stochastic process, and the observed fact that fluctuations of horizontal salinity gradients within the mixed layer on the 10-km scale are much larger than the critical value, the results of this statistical study has its own attractions. We have shown that the stochastic process can overpower a moderate steady component of forcing and drive the system back to critical. The stochastic model does not require sharp tuning to reach a critical state that approximates that of the present day observed state.

The formalism of the Fokker–Planck equation provides a useful condensed way of understanding and obtaining the statistical results. It leads to evaluation of integrals, as opposed to the alternative of a prolonged series of numerical time-stepping runs. Simple asymptotic approximations of these integrals are obtained for large-amplitude stochastic forcing. They afford maximum condensation of the statistical information that one desires from this model.

Acknowledgments. HMS's work at Woods Hole is supported by Grant OCE89-13128 from the National Science Foundation. WRY is supported Grant-OCE-9006430 from the National Science Foundation. We thank Lisa Stockinger for her assistance with the computations in this article.

REFERENCES

Abramowitz, M., and I. A. Stegun, 1972: *Handbook of Mathematical Functions and Formulas, Graphs and Mathematical Tables.* Wiley & Sons 1046+xiv pp.

Birchfield, G. E., 1989: A coupled ocean–atmosphere climate model: Temperature versus salinity effects on the thermohaline circulation. *Climate Dyn.,* **4,** 57–71.

Bryan, F., 1986: High-latitude salinity effects and interhemispheric thermohaline circulations. *Nature,* **323,** 310–304.

Marotzke, J., 1989: Instabilities and multiple steady states of the thermohaline circulation. *Ocean Circulation Models: Combining Data and Dynamics,* D. L. T. Anderson and J. Willebrand, Eds., Kluwer Academic, 501–511.

Risken, H., 1989: *The Fokker–Planck Equation.* 2d ed., *Springer Series in Synergetics,* No 18. Springer-Verlag, 472 pp.

Stommel, H., 1961: Thermohaline convection with two stable regimes of flow. *Tellus,* **13**(2), 224–230.

——, 1992: A conjectural regulating mechanism for determining the thermohaline structure of the oceanic mixed layer. *J. Phys. Oceanogr.,* **22,**

Taylor, G. I., 1921: Diffusion by continuous movements. *Proc. London Math. Soc.,* **20,** 196–212.

van Kampen, N. G., 1984: *Stochastic Processes in Physics and Chemistry.* Elsevier Science 419+xiv pp.

Wax, N. (Ed.), 1954: *Noise and Stochastic Processes,* Dover 337 pp.